Revising Geological Maps using RADARSAT *

Yan Shouxun and Vern Singhroy
Canada Centre for Remote Sensing, 588 Booth Street, Ottawa, Ontario K1A OY7
Phone number: 1-613-947-1326
Shouxun.yan@ccrs.nrcan.gc.ca
Vern.Singhroy@ccrs.nrcan.gc.cn

Abstract ***RADARSAT-1 images have been used to revise geological interpretations in three test sites. The sites are the rugged mountains in northern Hebei and the central Yunnan provinces in China, and the rugged mountainous rain forested terrains of the Guyana Shield. This case study demonstrates that careful interpretation of selective beam modes of RADARSAT-1 can add new structural and lithological information, thereby revising existing geological maps.***

Keywords: ***RADARSAT-1, Geological map revision, China, Guyana***

1. Introduction

Several studies have shown that SAR images provide useful information on topography, rock texture, moisture and surface material there by permitting lithological and structural mapping in difficult terrains (Ford *et al*., 1998, Sabins, 1996, Macdonald, 1980). RADARSAT-1 offers 35 different beam-mode combinations, with incidence angles ranging from 10 to 59 degrees, and spatial resolutions varying from 10 to 100m. Recently the relative benefits of the viewing geometry of RADARSAT-1 for geological mapping have been evaluated by Singhroy *et al.* (1999) and Budkewitsch (1997). In this paper we provide further evidence on using different beam modes for geological map revision in rugged areas. The test sites considered are:

- The rugged terrains (300-900m) hosting the Great Wall type gold ore deposit area in northern Hebei Province of China. The lithological units are Archean gneiss, Proterozoic to Low Paleozoic dolomite intercalated with sandstone, shale and marl; Middle Jurassic andesite and Mesozoic granite. RADARSAT-1, Standard mode, beam 2 with incidence angle 24^o–31^o, and resolution 25m was used for geological interpretation.
- The rugged forested terrains (1500-3000m) in the Jinshajiang river area of central Yunnan Province, southwestern China. The lithological units are Proterozoic gneiss and carbonate, clastic rocks, Paleozoic schist and Mesozoic clastic rocks. The RADARSAT-1 Fine mode, beam-3 with incidence angle 41^o-44^o and resolution of 8 m. was used for geological interpretation.
- The rugged tropical rain forested terrain (1000-3000m) of the Guyana Shield. The lithological units are greenstone belts with granites, basic intrusives and metavolcanics. RADARSAT-1, Wide mode1and 2, with incidence angles of 20^o-31^o and 31^o –39^o, and resolution of 30m were mosaiced for geological interpretation.

2. Geological Interpretation

The selection of the respective incidence angles was based on models developed by Singhroy and St-Jean (1999). The Wide mode 1 and 2 images of the Guyana Shield were mosaiced. All the SAR images have been processed and enhanced using techniques described by Singhroy (1996).

The *Great Wall type gold ore deposit* consisted of Archean granulite facies rocks representing the deepest crustal section in the northern China platform. Pyroxene granulite intercalated with biotite plagioclase gneiss and biotite plagioclase gneiss intercalated with pyroxene granulite, magnetite quartzite extensively distribute in south and west of the Great Wall type gold ore deposit area. During Proterozoic, an EW-trending rift developed on the bases of the Archean basement. Marine face dolomite intercalated with shale and sandstone sedimented in the rift basin. Cambrian – Ordovician basin limestone and shale locally distribute along the NE-trending faults occurring between the Archean and Proterozoic. During Mesozoic, continental extension and thrust and nappe movements happened

* *Presented at the 23rd Canadian Symposium on Remote Sensing, Quebec- August 21-24, 2001.*

alternatively. The Jurassic andesite and red granulite formed companying with the large granitic intrusives during extension. The andesite and red granulite locally distribute along the southern faults occurring between the Archean and Proterozoic. The NE-trending reverse faults generated during thrust and nappe movements in Mesozoic. Meanwhile, the SN-trending transverse faults formed to adjust the extensional and thrust movements.

Three kinds of lithologic terrains can be identified easily (Fig 1, Fig.2 and Table 1). They are Archean ganulite gneiss terrain, Proterozoic and Camberian to Ordovician dolomite terrain and Mesozoic granitic terrain. The intercalated

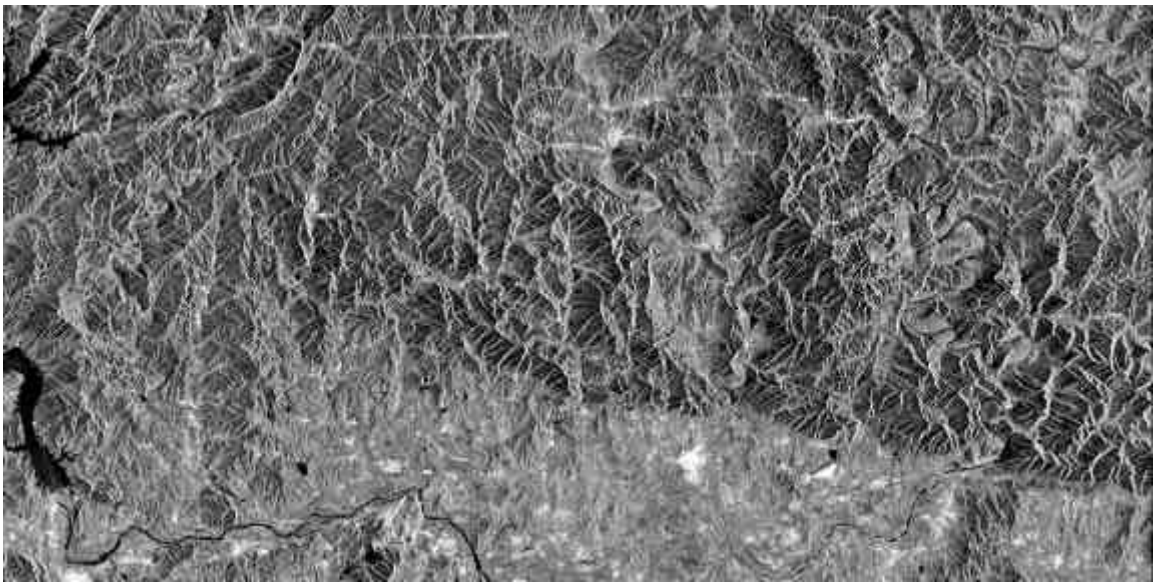

Fig.1. RADARSAT-1 image in the Great Wall type gold ore deposit area, Hebei province, P. R. China Desc. Orbit, 08-Oct-96, Standard mode, beam 2, Incidence angle: 24°-31°, Resolution: 25m.

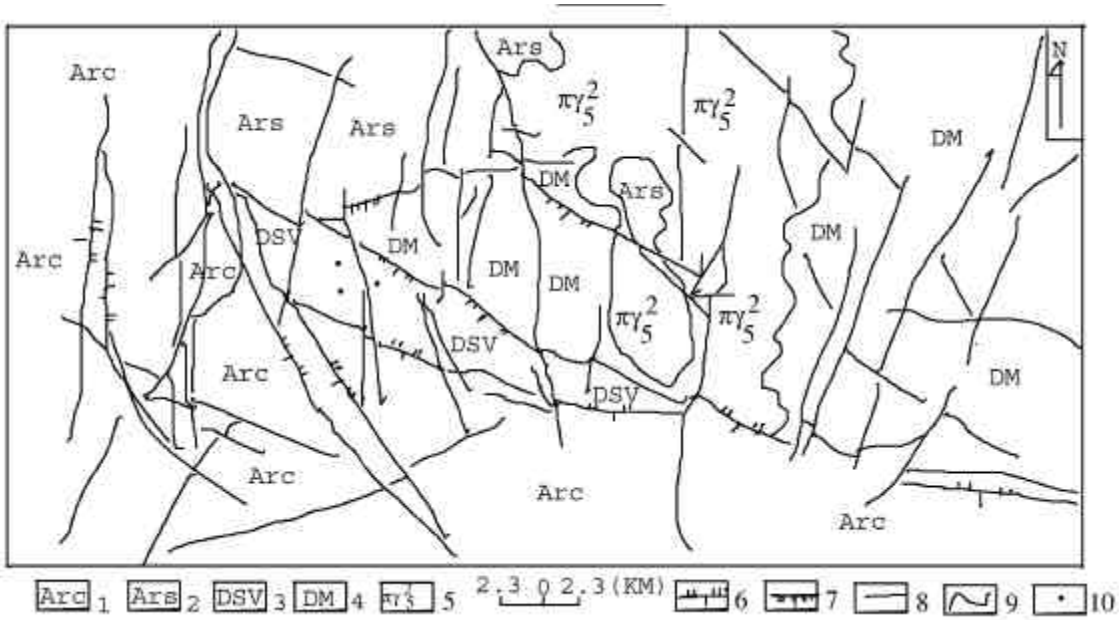

Fig.2. Geological interpretation map of SAR image in the Great Wall type gold ore deposit area, Hebei province, P. R. China

1-Archean pyroxene granulite interclated with biotite plagioclase gneiss; 2-Archean biotite plagioclase gneiss interclated with pyroxene granulite, magnetite quartze; 3 – Most of Lower Proterozoic dolomite and some of Middle Proterozoic dolomite, Cambrian-Ordovician limestone and shale, and Jurassic andesite.

4- Lower Proterozoic dolomite and quartzose sandstone; 5- Mesozoic po5rphyrite granite; 6 – Reverse fault; 7 – Normal fault; 8 – Fault; 9 – Geological line; 10 – Gold ore deposits.

beds of shale and sandstone and middle Jurussic andesite and red granulite cannot be identified because of thin-bedded and limited distribution. Furthermore, strata units from low Proterozoic to upper Proterozoic and to Camberian and Ordovician are all dolomites and cannot be subdivided.

We map the NE – SN trending reverse faults (Figs.1 and 2) and identify new SN-trending transverse faults. The faults interpreted from the SAR images are difficult to map in the field (Yan Shouxun *et al*., 1997, 1999, 2000), and as such the existing published maps are revised. There are close spatial and genetic relationships between the Great Wall type gold ore deposits and the NE-trending reverse faults, Proterozoic dolomite and the Mesozoic granite.

Table 1. The geological units and their interpretative key in the Great Wall type gold ore deposit area, north of the Hebei province, P. R. China

Geological units	Interpretative key
Arc: Archean pyroxene granulite interclated with biotite plagioclase gneiss	Brightest tone in lowest area due to vegetation and residence with smooth and sparkle textures. Middle grey light in moderate mountains with coarse texture.
Ars: Archean biotite plagioclase gneiss interclated with pyroxene granulite, magnetite quartzite	Moderate to dark grey light and coarse texture. Banded and arc ridges with high rugged topography.
DSV: Most of Low Proterozoic dolomite and some of Middle Proterozoic dolomite, Cambrian – Ordovician limestone and shale and Jurassic andesite	Dark tone and coarse texture. Strap block along faults with rugged high topography.
DM: Low Proterozoic dolomite and quartzose sandstone	Dark tone and coarse texture with rugged high topography
$\pi\lambda^2_5$: Mesozoic porphyritic granite	Bright tone and smooth to coarse texture. Oral and circular shapes with low to moderate topography.

The *Jinshajiang river area*, of Central Yunnan Province consisted of 3 classes of metamorphic rocks: the Proterozoic middle grade, the Sinian to Paleozoic low grade, and the Mesozoic very-low grade metamorphic rocks. Each unit has its own SAR visual characteristics with interpretation shown in (Figs. 3and 4). The RADARSAT-1 F3 image shows the lithological units, faults and folds. NS-, NE- and NW-trending faults are prominent. Folds with NNE-trending axes were superimposed on the later stage folds with EW-trending axes. The EW-trending fold in the Triassic strata (T) can also be identified.

Quaternary fault basins are not shown in the current geological map. Dislocations of the faults and the directions of fault-block displacement were interpreted from the fine mode image (Figs. 3 and 4). The NS-trending and NE-trending faults are strike-slip. During formation of the fault basins, the principal compression axis is NW-SE-trending, and the principal extensional axis is NE-SW- trending (Fig 4A)

Guyana Shield

Our research area is located in north of the Takuta graben in the Guyana shield (Gibbs *et al*., 1993). The area is covered with heavy rain forests with poor rock exposures (10-15%) and the deep weathered surficial cover. The relief closely follows the shield geology. Interpretation of the RADARSAT images shows the terrain and erosion surfaces are largely controlled by extensive block faulting. This is evident in the mesas of the Rorima Group, the ridges of the Avanavero Suite, the gabbro-noritic sills and dikes (Viskne *et al*., 1970; Miranda *et al*., 1991; Tonon *et al*., 1996; Singhroy *et al*, 1995). The major lithologic units are: the Proterozoic Greenstone belts (Barama-Mazaruni

Supergroup, PI); the Trans-Amazonian Tectonic-thermal episode grantites, makarapan riebeckite granite (rpI); the middle Proterozoic fluviate sand, chert mudstone (Muruwa Formation, PMm); the acid/intermediate volcanics(αPM) and the subvolcanic granites (rPM); fluviatile sands and conglomerates, thin bands of vitric tuff (Roraima Group, PMr); Gabbro-morite sills and dikes. These units were interpretated from the wide mode RADARSAT mosaic. This figure is too large to be included in this brief report, but is shown in the presentation together with the geological interpretative map.

Fig.3 RADARSAT-1 image in the Jinshajiang river area, central Yunnan province, southwestern P. R. China Asc. Orbit, 23-Oct-96, Fine mode, beam3, Incidence angle: 41^o-44^o, Resolution: 8m.

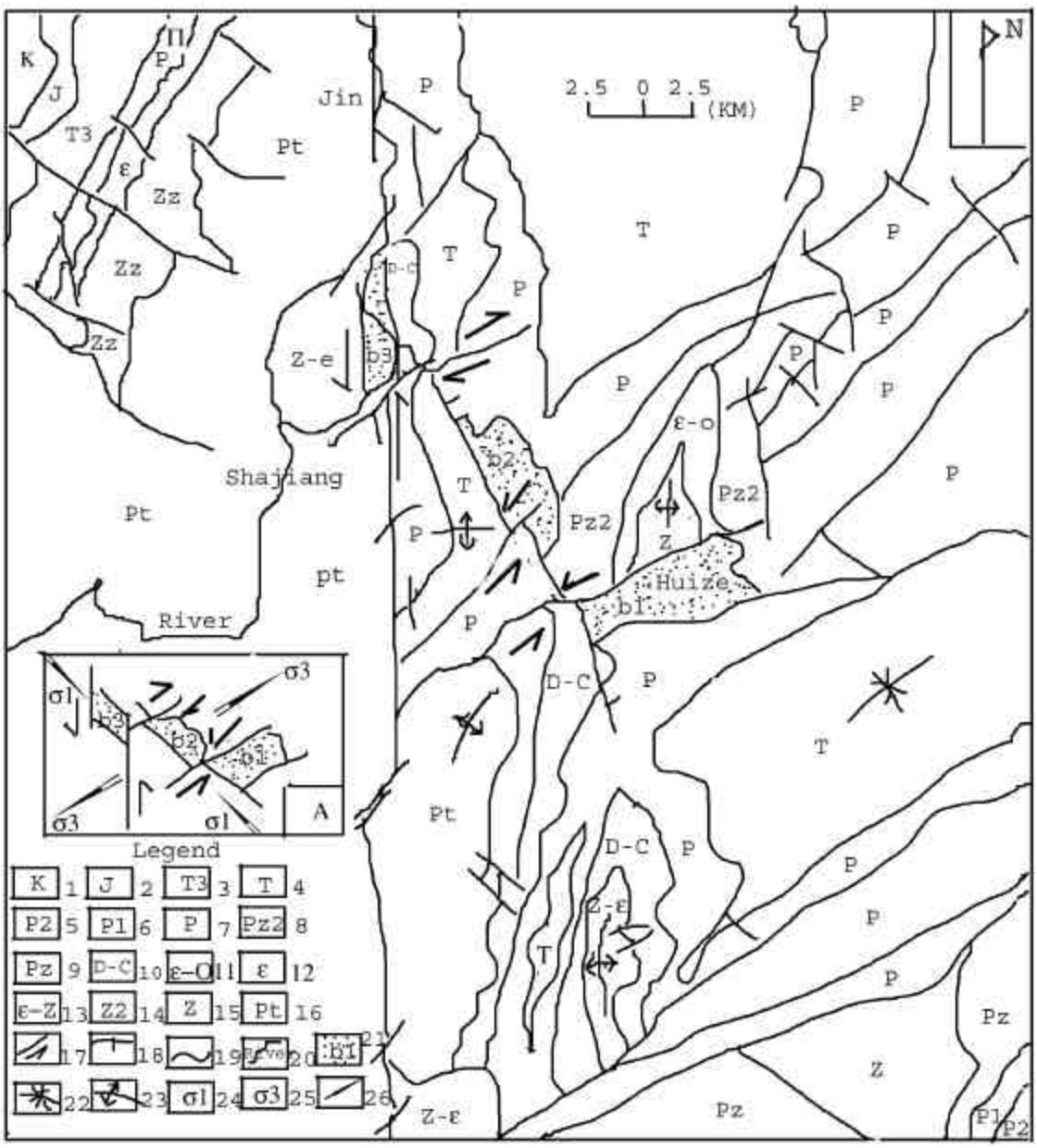

Fig.4 The geological interpretation map of SAR image in the Jinshajiang river area, central Yunnan province, southwestern P. R. China

1- Cretaceous purple clastic rocks; 2- Jurassic clastic rocks, intercalated with coal; 3- Upper Triassic clastic rocks, intercalated with limestone; 4- Triassic clastic rocks, limestone, intercalated with coal; 5- Upper permian carbonate, clastic rocks, intercalated with coal; 6- Lower Permian carbonate, clastic rocks; 7- Permian carbonate, clastic rocks, mostly basalt in the upper part; 8- Upper palaeozoic carbonate, clastic rocks, volcanic rocks, siliceous rocks; 9- Palaeozoic limestone and slate; 10- Devonian-Carboniferous low grade mata-clastic rocks, limestone; 11- Cambrian-Ordovician shale, intercalated with carbonate rocks; 12- Cambrian limestone; 13- Cambrian-Sinian slate, schist, intercalated with sandstone, quarzite, clastic rocks; 14- Upper Sinian carbonate, clastic rocks; 15- Sinian clastic, carbonate rocks; 16- Proterozoic gneiss, migmatite, amphibolite, marble; 17- Fault and its movement direction; 18- Normal fault; 19- Geological line; 20- Jinshajiang river; 21- b1-b3: fault basins; 22- Axis of syncline; 23- Axis of anticline; 24- Principal compression stress; 25- Principal extensional stress; 26- Direction of stresses. A- Geomechanic dynamic model of generation of the fault basins.

3. Summary

- RADARSAT-1 images are very useful for geological mapping in rugged mountains and forested terrain. But different beam mode with different resolutions of RADARSAT-1 images have different capabilities and limitation for identification of geological characteristics.
- In the Jinshajiang river the major lithological units and structures identified from the fine mode data. The framework of the Quaternary fault basins and their genesis were interpreted.
- The major geological terrains, Archean gneiss terrain, Proterozoic carbonate terrain and the Mesozoic granitic terrain were identified in the Great Wall type gold ore deposit area. It is difficult to subdivide strata units of different geological times among the dolomite terrain. The thin thickness Mesozoic andesite also can not be identified. Otherwise, many transverse structures have been recognised in the image, which can be used to revise the existing large scale (1:50 000) geological map.
- Wide beam mode images were used to identify the lithological units of the mountainous Middle Proterozoic terrain in northern Guyana shield. As the relief closely follows geology of the shield, most of the lithological units recognised in the image are confirmed with mapping units.

Acknowledgment

The authors gratefully acknowledge the support of Katrin Molch, Eric Gauthier, Patrick Assouad and Dongyi Li.

References

BUDKEWITSCH, P., D'Iorio, M., Wilkinson, L., Henderson J., 1997. Radar Images as a Source of Geological Information in Northern Barren Environments. International Symposium, Geomatics in the Ero of RADARSAT (GER'97), Ottawa, Canada, May 25-30, pp.7.

FLORD F. Sabins, 1996, Remote Sensing Principles and Interpretation, (Third edition) W. H. Freeman and Company, New York, pp.177-254.

GIBBS A. K., Barron, C. N., 1993, The Geology of the Guiana Shield. Oxford University Press.

GAYANA Geology and mines Commission, 1987, Geological Map of Guyana, Scale 1:1000000.

HAROLD C., MacDonald, 1980, Techniques and Applications of Image Radars, In: Berry S. Sieyal. Alanr. Gillespie (eds), Remote Sensing in Geology. John wiley & Sons. New York, Chichester, Brisbane, Toronto. pp.297-336.

JOHN P. Ford et al., 1998, Radar Geology. In: Floyd M. Henderson, Anthony J. Lewis (eds). Principles & Applications of Imaging Radar. Manual of Remote Sensing, Third Edition, Volume 2, Published in Coperation with the American Society for Photogrammetry and Remote Sensing. pp.511-565.

MIRANDA, F. P., J.V.Taranic, A.E.McCafferty, 1991, Identification of Terrane Categories and Geologic Structures Using SIR-B and Digital Aeromagnetic Data in the Rain Forest-Covered GuIana Shield, Northwestern Brazil. In: Proceedings of the Twenty-fourth International Symposium on Remote Sensing of Environment. Vol.I, 27-31 May 1991. pp.242-254.

SINGHROY. V. and R. Saint-Jean, 1999, Effects of Relirf on the Selection of Radarsat-1 Incidence Angle for Geological Application. Canadian Journal of Remote Sensing. Vol.25, No.3, PP. 211-217.

SINGHROY .V 1996 Environmental and Geological site characterization in vegetated areas: Image enhancement guidelines .Remote Sensing and GIS: Applications and Standards. ASTM Special Technical Publication #1279 . V. SINGHROY, D. Nebert. and A. Johnson, Eds., American Society for Testing and Materials. pp. 5-17.

SINGHROY. V, Rivard-benoit, Saint. J., 1995, SAR Integration Techniques for Geological Investigations, Case Studies in Jordan, Canada andf Guyana. In: Epp-Helmut and Taylor-Cindy (eds.), Proceedings of the Seventeenth Canadian Symposium on Remote Sensing; Radar Remote Sensing; A tool for Real-time Land Cover Monitoring and GIS Integration. pp.734-841.

TONON-M, Cantou-J-P, Gigord-P, Sylvander-S, de-Gaujac-A-C, 1996, Map Coverage of French Guyana by Space Trisngulation of Images. In: ERS applications. ESA SP. Euoropean Space Agency Special Publication. 383, pp.369-372.

VISKNE, A., T. C. Liston, and C. D. Sapp, 1970. SLA Reconnaissance of Panama. Photogrammetric Engineering, Vol.36, No.3, pp. 253-269.

YAN Shouxun et al. 1999, Transverse Structure. In: Ma Zhongjin(edit), New Progress of Tectonic Dynamics and Lithosphere Dynamics. Seismic Press, pp.157-163 (Chinese with English abstract).
YAN Shouxun et al., 1997, On Adjustment Structure. Scientai Geologica Sinica, Vol.32, No.2, pp.146-155(in Chinese with English abstract).
YAN Shouxun, Zhu Zhenghai, Huang Xiaoxia, 2001, Remote Sensing and Aeromagnetic Anomaly Integration Analysis of Transverse Structure and its Ore-controlling Significance, Journal of Remote Sensing, (Chinese with english abstraction. In press)